Scientia Iranica B (2013) 20(4), 1241–1253

SCIENTIA IRANICA

Sharif University of Technology
**Scientia Iranica**
*Transactions B: Mechanical Engineering*
www.scientiairanica.com

# Natural convection in a nanofluid filled concentric annulus between an outer square cylinder and an inner elliptic cylinder

**M. Sheikholeslami***, **M. Gorji-Bandpy and D.D. Ganji**

*Department of Mechanical Engineering, Babol University of Technology, Babol, Iran.*

Received 25 April 2012; received in revised form 10 February 2013; accepted 6 May 2013

**KEYWORDS**
Elliptic cylinder;
Natural convection;
Lattice Boltzmann method;
Nanofluid;
Concentric annulus.

**Abstract.** The lattice Boltzmann method is applied to investigate the natural convection flow of a nanofluid in a concentric annulus between a cold outer square cylinder and a heated inner elliptic cylinder. In order to simulate the effective thermal conductivity and viscosity of nanofluid, Maxwell-Garnetts (MG) and Brinkman models are used, respectively. This investigation is compared with other numerical methods and found to be in excellent agreement. Numerical results for flow and heat transfer characteristics are obtained for various values of the nanoparticle volume fraction, Rayleigh number and eccentricity. The results show that the minimum value of enhancement of heat transfer occurs at $\varepsilon = 0.95$ for $\mathrm{Ra} = 10^5$, but, for other values of Rayleigh number, is obtained at $\varepsilon = 0.65$.



## 1. Introduction

The low thermal conductivity of conventional heat transfer fluids, such as water, is considered a primary limitation in enhancing the performance and compactness of such thermal systems. An innovative technique for improving heat transfer by adding nano-scale particles in the base fluids has been used extensively during the last decade. The term nanofluid refers to those kinds of fluid which have nano-scale particles suspended in the base fluid [1]. Khanafer et al. [2] investigated a numerical study on heat transfer enhancement due to adding nano-particles in a differentially heated enclosure. They found that the suspended nanoparticles substantially increase the heat transfer rate at any given Grashof number. Abu-Nada and Oztop [3] analyzed the effects of inclination angle on natural convection heat transfer and fluid flow in a two-dimensional enclosure filled with Cu-nanofluid. They reported that the inclination angle can be a control parameter for a nanofluid filled enclosure. Oztop and Abu-Nada [4] studied natural convection in partially heated rectangular enclosures filled with nanofluids. They showed that the heat transfer enhancement, using nanofluids, is more pronounced at low aspect ratio than at high aspect ratio. Oztop et al. [5] used Heatline visualization technique to understand the heat transport path in an inclined non-uniformly heated enclosure filled with water based CuO nanofluid. They showed that heat transfer in the cavity increases by adding nanoparticles. However, the rate of increase is greater for the enclosures with low Rayleigh numbers in which conduction heat transfer is more dominant. Sheikholeslami et al. [6] studied magnetohydrodynamic flow in a nanofluid filled inclined enclosure with a sinusoidal wall. They reported that for all values of Hartmann number, at $\mathrm{Ra} = 10^4$ and $10^5$, maximum values of enhancement are obtained at $\gamma = 60°$ and $\gamma = 0°$, respectively. Soleimani et al. [7] applied a Control Volume based Finite Element Method to investigate

*. *Corresponding author. Tel: +98 911 3968030*
*E-mail address: mohsen.sheikholeslami@yahoo.com (M. Sheikholeslami)*

the natural convection heat transfer in a semi-annulus enclosure filled with nanofluid. They found that the angle of turn has an important effect on the streamlines, isotherms and maximum or minimum values of local Nusselt number. Abu-Nada et al. [8] investigated natural convection heat transfer enhancement in horizontal concentric annuli fields by nanofluid. They found that for low Rayleigh numbers, nanoparticles with higher thermal conductivity cause more enhancement in heat transfer. Oztop et al. [9] used heating and cooling by sinusoidal temperature profiles on one side of an enclosure filled with a nanofluid. They concluded that the addition of nanoparticles into water affects the fluid flow and temperature distribution. Nemati et al. [10] used the Lattice Boltzmann Method to investigate the effect of CuO nanoparticles on natural convection with MHD flow in a square cavity. They showed that the averaged Nusselt number increases for nanofluids when increasing the solid volume fraction, while, in the presence of a high magnetic field, this effect decreases. Abu-Nada et al. [11] performed a numerical study on natural convection for a water-CuO nanofluid filled enclosure. They showed that the location of maximum enhancement in heat transfer was sensitive to Rayleigh number, length of partial convection and volume fraction of the nanoparticle. Heat transfer of a nanofluid flow which is squeezed between parallel plates was investigated by Sheikholeslami and Ganji [12]. They reported that Nusselt number has a reverse relationship with the squeeze number when two plates are squeezed. Recently, several numerical studies have been carried out to simulate nanofluid thermal behavior [13-19].

In recent years, natural convective heat transfer in horizontal annuli has been of interest to many researchers because of its wide applications, such as in nuclear reactor design, cooling of electronic equipment, aircraft cabin insulation and thermal storage system. A large and diverse amount of literature on both experimental and numerical investigations has been published in the past few decades, the majority of which was involved in horizontal circular annuli. Natural convective heat transfer in horizontal annuli between two concentric circular cylinders has been well studied. The effect of surface radiation on conjugate natural convection in a horizontal annulus driven by an inner heat generating solid cylinder was investigated by Shaija and Narasimham [20]. Their results showed that surface radiation reduces the convective heat transfer in the annulus compared to the case of pure natural convection and enhances the overall Nusselt number. Onyegegbu [21] analytically studied heat transfer in an absorbing and emitting non-gray Boussinésq fluid within the annular gap of two infinitely long isothermal horizontal concentric cylinders using the Milne-Eddington approximation. He observed that surface radiation reduces the convective heat transfer in the annulus compared to pure natural convection. Sheikholeslami et al. [22] performed a numerical analysis for natural convection heat transfer of Cu-water nanofluid in a cold outer circular enclosure containing a hot inner sinusoidal circular cylinder in the presence of a horizontal magnetic field. They concluded that in the absence of a magnetic field, the enhancement ratio decreases as Rayleigh number increases, while an opposite trend is observed in the presence of a magnetic field. Haldar [23] reported a numerical study of combined convection through a horizontal concentric annulus using a combination of a vorticity-stream function and primitive variables formulations. It was found that by increasing axial distance, the entry effect diminishes, while the buoyancy becomes stronger. Efficient computation of natural convection in a concentric annulus between an outer square cylinder and an inner circular cylinder was undertaken by Shu and Zhu [24]. They found that both the aspect ratio and the Rayleigh number are critical to the patterns of flow and thermal fields.

The Lattice Boltzmann Method (LBM) (or Thermal Lattice Boltzmann Method (TLBM)) is a class of computational fluid dynamics (CFD) methods for fluid simulation. Instead of solving the Navier-Stokes equations, the discrete Boltzman is solved to simulate the flow of a Newtonian fluid with collision models such as Bhatnagar-Gross-Krook (BGK). By simulating streaming and collision processes across a limited number of particles, the intrinsic particle interactions evince a microcosm of viscous flow behavior applicable across the greater mass. LBM is a relatively new simulation technique for complex fluid systems and has attracted interest from researchers in computational physics. Unlike the traditional CFD methods, which solve the conservation equations of macroscopic properties (i.e., mass, momentum and energy) numerically, LBM models the fluid consisting of fictive particles, which perform consecutive propagation and collision processes over a discrete lattice mesh. Due to its particulate nature and local dynamics, LBM has several advantages over other conventional CFD methods, especially in dealing with complex boundaries, incorporating microscopic interactions, and parallelization of the algorithm [25,26]. Various numerical simulations have been performed using different thermal LB models or Boltzmann-based schemes to investigate natural convection problems [27-29]. Natural convection between a square outer cylinder and a heated elliptic inner cylinder has been studied numerically by Bararnia et al. [30]. They found that streamlines, isotherms, and the number, size and formation of the vortices strongly depend on Rayleigh number and the position of the inner cylinder. Kefayati et al. [31] studied the effect of $SiO_2$/water nanofluid for heat transfer improvement in tall enclosures using the lattice

Boltzmann method. They showed that the average Nusselt number increases with volume fraction for the whole range of Rayleigh numbers and the aspect ratios. They also showed that the effect of nanoparticles on heat transfer augments as the enclosure aspect ratio increases. Bararnia et al. [32] studied natural convection in a nanofluid filled portion cavity with a heated built-in plate by LBM. Their results have been obtained for different inclination angles and lengths of the inner plate. Sheikholeslami et al. [33] investigated natural convection in a concentric annulus between a cold outer square and heated inner circular cylinders in the presence of a static radial magnetic field. They reported that average Nusselt number is an increasing function of the nanoparticle volume fraction as well as Rayleigh number, while it is a decreasing function of Hartmann number. In recent years, some researchers have used new methods to solve these kinds of problems [34-36].

The purpose of the present paper is to study the natural convection of nanofluid in a cold outer circular enclosure containing a hot inner elliptic cylinder using the lattice Boltzmann method. The numerical investigation is carried out for different governing parameters, such as Rayleigh number, eccentricity and nanoparticle volume fraction.

## 2. Problem definition and mathematical model

### *2.1. Problem definition*

The physical model used in this work is shown in Figure 1. The model consists of a concentric annulus between a cold outer square cylinder with temperature $T_c$ and a heated inner horizontal elliptic cylinder with temperature $T_h$ ($T_h > T_c$). Setting $a$ as the major axis and $b$ as the minor axis of the elliptic cylinder, the eccentricity ($\varepsilon$) for the inner cylinder is defined as:

$$\varepsilon = \sqrt{a^2 - b^2}\Big/a \quad \text{or} \quad b = \sqrt{1-\varepsilon^2}.a. \tag{1}$$

In this study, for the inner ellipse, the major axis is $a = 0.4$ and the eccentricity varies from 0.65 to 0.95.

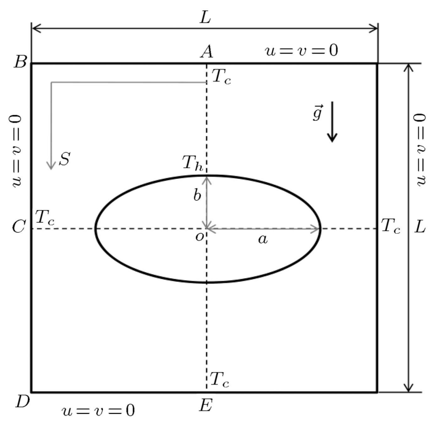


**Figure 1.** Geometry of the problem.

### *2.2. The lattice boltzmann method*

The LB model used here is the same as that employed in [27]. The thermal LB model utilizes two distribution functions, $f$ and $g$, for the flow and temperature fields, respectively. It uses modeling of the movement of fluid particles to capture macroscopic fluid quantities, such as velocity, pressure and temperature. In this approach, the fluid domain is discretized to uniform Cartesian cells. Each cell holds a fixed number of distribution functions, which represent the number of fluid particles moving in these discrete directions. The D2Q9 model was used and values of $w_0 = 4/9$ for $|c_0| = 0$ (for the static particle), $w_{1-4} = 1/9$ for $|c_{1-4}| = 1$ and $w_{5-9} = 1/36$ for $|c_{5-9}| = \sqrt{2}$ are assigned in this model (Figure 2(a)).

The density and distribution functions i.e. the $f$ and $g$, are calculated by solving the Lattice Boltzmann Equation (LBE), which is a special discretization of the kinetic Boltzmann equation. After introducing Bhatnagar-Gross-Krook approximation, the general form of the lattice Boltzmann equation with external force is as follows:

For the flow field:

$$f_i(x+c_i\Delta t, t+\Delta t) = f_i(x,t) + \frac{\Delta t}{\tau_v}[f_i^{eq}(x,t) - f_i(x,t)] + \Delta t c_i F_k. \tag{2}$$

For the temperature field:

$$g_i(x+c_i\Delta t, t+\Delta t) = g_i(x,t) + \frac{\Delta t}{\tau_C}[g_i^{eq}(x,t) - g_i(x,t)], \tag{3}$$

where $\Delta t$ denotes lattice time step, $c_i$ is the discrete lattice velocity in direction $i$, $F_k$ is the external force in the direction of the lattice velocity, and $\tau_v$ and $\tau_C$ denote the lattice relaxation time for the flow and

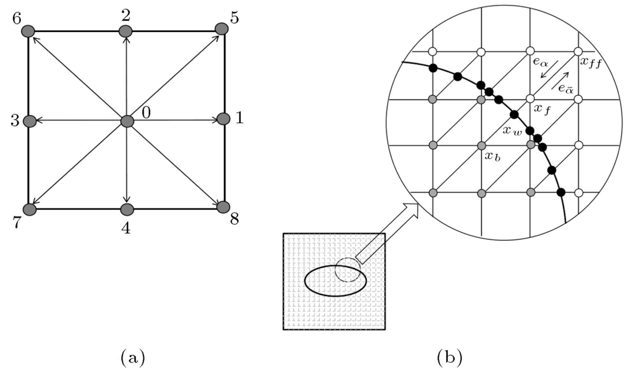


**Figure 2.** (a) Discrete velocity set of two-dimensional nine-velocity (D2Q9) model. (b) Curved boundary and lattice nodes.

temperature fields. Kinetic viscosity, $\upsilon$, and Thermal diffusivity, $\alpha$, are defined in terms of their respective relaxation times, i.e. $\upsilon = c_s^2(\tau_v - 1/2)$ and $\alpha = c_s^2 = (\tau_C - 1/2)$, respectively. Note that limitation $0.5 < \tau$ should be satisfied for both relaxation times to ensure that viscosity and thermal diffusivity are positive. Furthermore, the local equilibrium distribution function determines the type of problem that needs to be solved. It also models the equilibrium distribution functions, which are calculated with Eqs. (4) and (5) for flow and temperature fields, respectively.

$$f_i^{eq} = w_i\rho\left[1+\frac{c_i.u}{c_s^2}+\frac{1}{2}\frac{(c_i.u)^2}{c_s^4}-\frac{1}{2}\frac{u^2}{c_s^2}\right], \tag{4}$$

$$g_i^{eq} = w_i T\left[1+\frac{c_i.u}{c_s^2}\right], \tag{5}$$

where $w_i$ is a weighting factor and $\rho$ is the lattice fluid density.

In order to incorporate buoyancy forces in the model, the force term in Eq. (2) needs to be calculated, as below, in a vertical direction ($y$):

$$F = 3w_i g_y \beta\theta. \tag{6}$$

For natural convection, the Boussinesq approximation is applied and radiation heat transfer is negligible. To ensure that the code works in a near incompressible regime, the characteristic velocity of the flow for a natural ($V_{\text{natural}} = \sqrt{\beta g_y \Delta T H}$) regime must be small compared with the fluid speed of sound. In the present study, the characteristic velocity is selected as 0.1 of the sound speed.

Finally, macroscopic variables are calculated with the following formula (Figure 3):

$$\text{Flow density}: \quad \rho = \sum_i f_i,$$

$$\text{Momentum}: \quad \rho \mathrm{u} = \sum_i \mathrm{c}_i f_i,$$

$$\text{Temperature}: \quad T = \sum_i g_i. \tag{7}$$

### 2.3. Boundary conditions

#### 2.3.1. Curved boundary treatment for velocity

For treating velocity and temperature fields with curved boundaries, the method proposed in [37] has been used. An arbitrary curved wall separating the solid region from the fluid is shown in Figure 2(b). The link between the fluid node, $x_f$, and the wall node, $x_w$, intersects the physical boundary at $x_b$. The fraction of the intersected link in the fluid region is $\Delta = |x_f - x_w| / |x_f - x_b|$. To calculate the post-collision distribution function, $\tilde{f}_{\bar{\alpha}}(x_b, t)$, based upon the surrounding nodes information, a Chapman-Enskog expansion for the post-collision distribution function on the right-hand side of Eq. (2) is conducted as:

$$\tilde{f}_{\bar{\alpha}}(x_b,t) = (1-\chi)\tilde{f}_\alpha(x_f,t) + \chi f_\alpha^*(x_b,t) + 2w_\alpha\rho\frac{3}{c^2}\mathrm{e}_{\bar{\alpha}}.\mathrm{u}_w, \tag{8}$$

where:

$$f_\alpha^*(x_b,t) = f_\alpha^{eq}(x_f,t) + w_\alpha\rho(x_f,t)\frac{3}{c^2}e_\alpha.(u_{bf}-u_f),$$

$$\mathrm{u}_{bf} = \mathrm{u}_{ff} = u(x_{ff},t), \qquad \chi = \frac{(2\Delta-1)}{\tau-2},$$

$$\text{if } 0 \le \Delta \le \frac{1}{2},$$

$$\mathrm{u}_{bf} = \frac{1}{2\Delta}(2\Delta-3)u_f + \frac{3}{2\Delta}u_w, \quad \chi = \frac{(2\Delta-1)}{\tau-1/2},$$

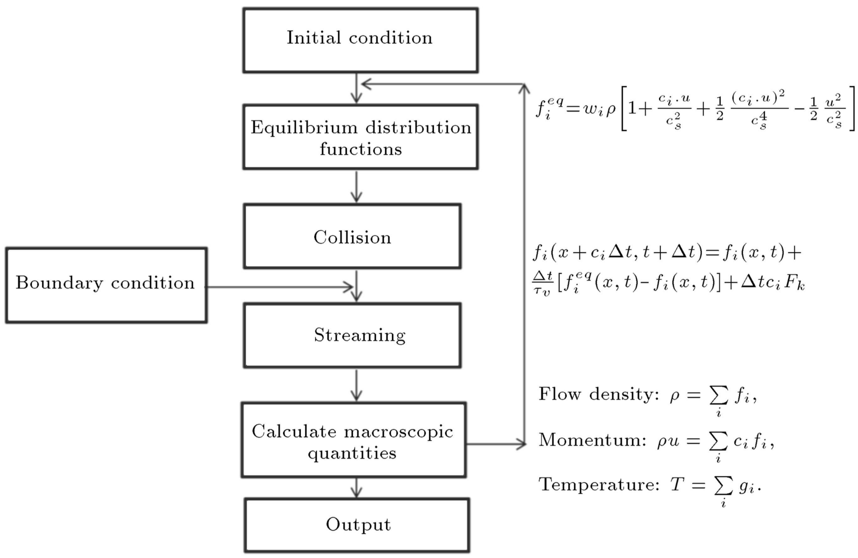


**Figure 3.** Algorithm flowchart of Lattice Boltzmann Method.

**Table 1.** Thermo physical properties of water and nanoparticles [2].

| | $\rho$ (kg/m$^3$) | $C_p$ (j/kgk) | $k$ (W/m.k) | $\beta \times 10^5$ (k$^{-1}$) |
|---|---|---|---|---|
| Pure water | 997.1 | 4179 | 0.613 | 21 |
| Copper (Cu) | 8933 | 385 | 401 | 1.67 |

$$\text{if } \frac{1}{2} \leq \Delta \leq 1. \tag{9}$$

In the above, $e_{\bar{\alpha}} \equiv -e_\alpha; u_f$ is the fluid velocity near the wall; $u_w$ is the velocity of the solid wall and $u_{bf}$ is an imaginary velocity for interpolations.

*2.3.2. Curved boundary treatment for temperature*

Following the work of Yan and Zu [37], the non equilibrium parts of the temperature distribution function can be defined as:

$$g_{\bar{\alpha}}(\mathbf{x}_b, t) = g_{\bar{\alpha}}^{eq}(\mathbf{x}_b, t) + g_{\bar{\alpha}}^{neq}(\mathbf{x}_b, t). \tag{10}$$

Substituting Eq. (10) into Eq. (3) leads to:

$$\tilde{g}_{\bar{\alpha}}(\mathbf{x}_b, t + \Delta t) = g_{\bar{\alpha}}^{eq}(\mathbf{x}_b, t) + (1 - \frac{1}{\tau_s})g_{\bar{\alpha}}^{neq}(\mathbf{x}_b, t). \tag{11}$$

Obviously, both $g_{\bar{\alpha}}^{eq}(\mathbf{x}_b, t)$ and $g_{\bar{\alpha}}^{neq}(\mathbf{x}_b, t)$ are needed to calculate the value of $\tilde{g}_{\bar{\alpha}}(\mathbf{x}_b, t + \Delta t)$. In Eq. (11), the equilibrium part is defined as:

$$g_{\bar{\alpha}}^{eq}(\mathbf{x}_b, t) = w_{\bar{\alpha}} T_b^* \left(1 + \frac{3}{c^2}\mathbf{e}_{\bar{\alpha}}.\mathbf{u}_b^*\right), \tag{12}$$

where $T_b^*$ is defined as a function of $T_{b1} = [T_w + (\Delta - 1)T_f]/\Delta$ and $T_{b2} = [2T_w + (\Delta - 1)T_{ff}]/(1 + \Delta)$.

$$\begin{aligned} T_b^* &= T_{b1}, && \text{if } \Delta \geq 0.75, \\ T_b^* &= T_{b1} + (1 - \Delta)T_{b2}, && \text{if } \Delta \leq 0.75, \end{aligned} \tag{13}$$

and $u_b^*$ is defined as a function of $u_{b1} = [u_w + (\Delta - 1)u_f]/\Delta$ and $u_{b2} = [2u_w + (\Delta - 1)u_{ff}]/(1 + \Delta)$.

$$\begin{aligned} u_b^* &= u_{b1}, && \text{if } \Delta \geq 0.75, \\ u_b^* &= u_{b1} + (1 - \Delta)u_{b2}, && \text{if } \Delta \leq 0.75. \end{aligned} \tag{14}$$

The non equilibrium part in Eq. (15) is defined as:

$$g_{\alpha}^{neq}(\mathbf{x}_b, t) = \Delta g_{\alpha}^{neq}(x_f, t) + (1 - \Delta)g_{\alpha}^{neq}(x_{ff}, t). \tag{15}$$

### *2.4. The Lattice Boltzmann model for nanofluid*

In order to simulate the nanofluid by the lattice Boltzmann method, because of interparticle potential and other forces on the nanoparticles, the nanofluid behaves differently from pure liquid, from a mesoscopic point of view, and has higher efficiency in energy transportation, as well as better stabilization, than the common solid-liquid mixture. For pure fluid, in the absence of nanoparticles in the enclosures, the governed equations are Eqs. (2)-(15). However, for modeling the nanofluid, because of changes in the fluid thermal conductivity, density, heat capacitance and thermal expansion, some governed equations should change.

The fluid in the enclosure is Cu-water nanofluid. The nanofluid is a two component mixture with the following assumptions: (i) incompressibility; (ii) no-chemical reaction; (iii) negligible viscous dissipation; (iv) negligible radiative heat transfer; (v) nano-solid-particles and the base fluid are in thermal equilibrium and no slip occurs between them. The thermo physical properties of the nanofluid are given in Table 1 [2].

The effective density, $\rho_{nf}$, the effective heat capacity, $(\rho C_p)_{nf}$, and thermal expansion, $(\rho\beta)_{nf}$, of the nanofluid are defined as [38]:

$$\rho_{nf} = \rho_f(1 - \phi) + \rho_s\phi, \tag{16}$$

$$(\rho C_p)_{nf} = (\rho C_p)_f (1 - \phi) + (\rho C_p)_s \phi, \tag{17}$$

$$(\rho\beta)_{nf} = (\rho\beta)_f (1 - \phi) + (\rho\beta)_s \phi, \tag{18}$$

where $\phi$ is the solid volume fraction of the nanoparticles, and subscripts $f$, $nf$ and $s$, stand for base fluid, nanofluid and solid, respectively.

The viscosity of the nanofluid containing a dilute suspension of small rigid spherical particles is (Brinkman model [39]):

$$\mu_{nf} = \frac{\mu_f}{(1 - \phi)^{2.5}}. \tag{19}$$

The effective thermal conductivity of the nanofluid can be approximated by the Maxwell-Garnetts (MG) model as [2]:

$$\frac{k_{nf}}{k_f} = \frac{k_s + 2k_f - 2\phi(k_f - k_s)}{k_s + 2k_f + \phi(k_f - k_s)}. \tag{20}$$

In order to compare total heat transfer rate, a Nusselt number is used. The local and average Nusselt numbers are defined as follows:

$$\mathrm{Nu}_{loc} = \frac{k_{nf}}{k_f}\frac{\partial T}{\partial n} \quad \text{and} \quad \mathrm{Nu}_{ave} = \frac{1}{L}\int_0^L \mathrm{Nu}dS. \tag{21}$$

The relaxation time for flow $(\tau_v)$ is defined as: $\tau_v = (3\upsilon + 0.5)$. The relaxation time for temperature $(\tau_C)$ is defined as: $\tau_C = (3\alpha_{nf} + 0.5)$, where $\alpha_{nf} = \upsilon \mathrm{Pr}_{nf}$

and $\Pr_{nf} = \mu_{nf}(C_p)_{nf}/k_{nf}$. Also, by fixing the Rayleigh number, Prandtl number and Mach number, the viscosity is calculated from the definition of $\upsilon = \sqrt{\mathrm{Ma}^2 L^2 \Pr_{nf} c_s^2/\mathrm{Ra}}$, where $L$ is the number of lattices in the $y$-direction (parallel to gravitational acceleration). This Mach number should be less than 0.3 to insure an incompressible flow. Therefore, Mach number was fixed at $\mathrm{Ma} = 0.1$ in the present study.

## 3. Grid testing and code validation

To verify the grid independence of the solution scheme, numerical experiments are performed, as shown in Table 2. Different mesh sizes were used for the case of RA $= 10^6$, $a = 0.4$, $\varepsilon = 0.95$ and $\phi = 0.06$. The present code is tested for grid independence by calculating the average Nusselt number on the outer wall. It is found that a grid size of $200 \times 200$ ensures the grid independent solution for the present case. The convergence criterion for the termination of all computations is:

$$\max_{grid} \left|\Gamma^{n+1} - \Gamma^n\right| \leq 10^{-7}, \tag{22}$$

where $n$ is the iteration number and $\Gamma$ stands for the independent variables $(U, V, T)$. The present numerical solution is validated by comparing the present code results against the results of Moukalled and Acharya [40] for viscous flow ($\phi = 0$). This comparison is presented in Table 3. Furthermore, another validation test was carried for natural convection in an enclosure filled with Cu-water for different Grashof numbers with the results of Khanafer et al. [2] in Figure 4. All previous comparisons indicate the accuracy of the present LBM code.

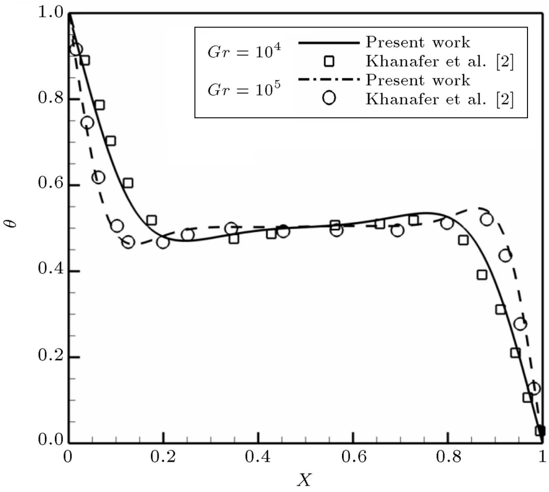


**Figure 4.** Comparison of the temperature on axial midline between the present results and numerical results by Khanafer et al. [2]; $\phi = 0.1$ and pr $= 6.8$ (Cu-water).

## 4. Results and discussion

Natural convection in a concentric annulus between a cold outer square cylinder and a heated inner elliptic filled with nanofluid is investigated numerically using the LBM. The fluid in the enclosure is Cu-water nanofluid. Calculations are made for different values of volume fraction of nanoparticle ($\phi = 0$, 0.02, 0.04 and 0.06), Rayleigh number (Ra $= 10^3, 10^4, 10^5$ and $10^6$) and eccentricity ($\varepsilon = 0.65, 0.8$ and 0.95) when the Prandtl number is fixed ($\Pr = 6.8$) and the major axis is $a = 0.4$.

The effects of Cu nanoparticles on the streamlines and isotherms are shown in Figure 5. As seen, the flow intensity increases with an increase in nanoparticle volume fraction, which enhances the energy transport within the fluid. Hence, the absolute values of the stream function, which represent the strength of flow, increase with increasing the volume fraction of the nanofluid (Figure 5). The sensitivity of the thermal boundary layer thickness to the volume fraction of the nanoparticles is related to the increased thermal conductivity of the nanofluid. In fact, higher values of thermal conductivity are accompanied by higher values of thermal diffusivity. The high value of thermal

**Table 2.** Comparison of the average Nusselt number along the surface of the inner cylinder $\mathrm{Nu}_{ave}$ for different grid resolution at Ra $= 10^6$, $a = 0.4$, $\varepsilon = 0.95$ and $\phi = 0.06$.

| **Mesh size** | $180 \times 180$ | $190 \times 190$ | $200 \times 200$ | $210 \times 210$ | $220 \times 220$ |
|---|---|---|---|---|---|
| $\mathbf{Nu}_{ave}$ | 6.107132 | 5.932234 | 5.778325 | 5.766139 | 5.74064 |

**Table 3.** Comparison of the average Nusselt number between the present results and numerical results obtained by Moukalled and Acharya [40] for pure fluid ($\phi = 0$) at $\Pr = 0.71$.

| | $\mathbf{10^4}$ | | $\mathbf{10^5}$ | | $\mathbf{10^6}$ | |
|---|---|---|---|---|---|---|
| $\boldsymbol{\lambda}$ | **Present work** | **Moukalled and Acharya [40]** | **Present work** | **Moukalled and Acharya [40]** | **Present work** | **Moukalled and Acharya [40]** |
| 5 | 2.07725 | 2.071 | 3.81596 | 3.825 | 6.12191 | 6.107 |
| 2.5 | 3.32386 | 3.331 | 5.0901 | 5.08 | 9.3938 | 9.374 |

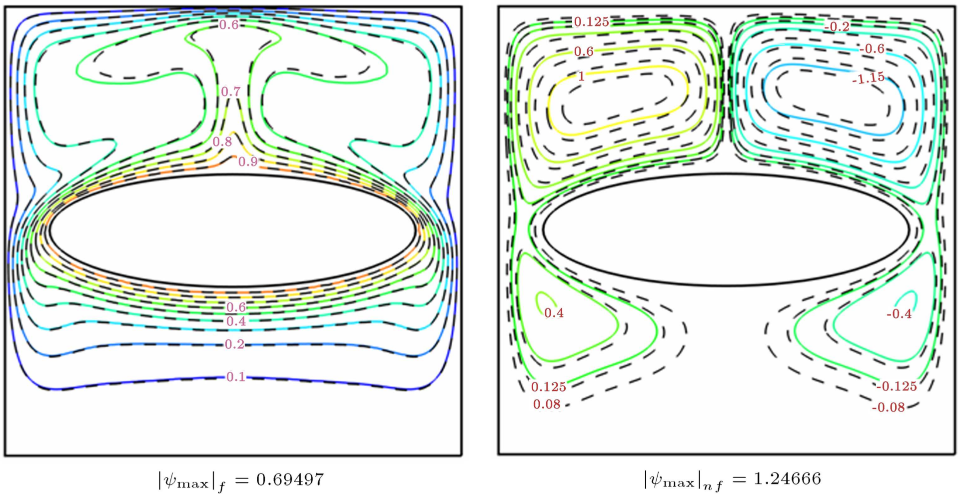


**Figure 5.** Comparison of the isotherms (left) and streamlines (right) contours between nanofluid ($\phi = 0.06$) (——) and pure fluid ($\phi = 0$) (– – –) for Ra = $10^6$ and $\phi = 0.06$.

diffusivity leads to an increase in thermal boundary layer thickness. However, the Nusselt number is a multiplication of temperature gradient and thermal conductivity ratio (conductivity of the nanofluid to the conductivity of the base fluid). Since the reduction in temperature gradient due to the presence of nanoparticles is much smaller than the thermal conductivity ratio, an enhancement in Nusselt takes place by increasing the volume fraction of the nanoparticles.

Effects of Ra and $\varepsilon$ on isotherm (up) and streamline (down) contours for the case of Cu-water ($\phi = 0.06$) is shown in Figure 6. As seen, the absolute value of maximum stream function increases with an increase in Rayleigh number and eccentricity. It can be observed that the flow and temperature contours are generally symmetrical about the vertical centre line of the inner circular cylinder. At Ra = $10^3$, the heat transfer in the enclosure is mainly dominated by the conduction mode, and the flow circulation shows two overall rotating symmetric eddies with two inner vortices in each half of the enclosure. At Ra = $10^4$, the patterns of isotherms and streamlines are about the same as those for Ra = $10^3$. As the Rayleigh number increases up to $10^5$, the role of convection in heat transfer becomes more significant and, consequently, the thermal boundary layer on the bottom surface of the inner cylinder becomes thinner. Also, a plume starts to appear on the top of the inner cylinder. In consequence, the dominant flow is in the upper half of the enclosure, and, correspondingly, the core of the recalculating eddies is located only in the upper half. At Ra = $10^6$ , a strong plume derives whose flow strongly impinges on the top of the enclosure. Thus, thermal boundary layer thickness decreases in this region. For $\varepsilon = 6.5$ and low Rayleigh numbers, Ra = $10^3$ and $10^4$, the isotherms and streamlines behave similar to those other values of $\varepsilon$. As the Rayleigh number increases up to Ra = $10^5$ and $10^6$, isotherms at the upper half of the enclosure are slightly squeezed and the temperature value at the vertical center line is lower than that at the same height close to the vertical centerline. Thus, the primary plume is divided into three plumes. Two upwelling plumes appear on the top of the inner cylinder. A third plume appears above the top of the inner circular cylinder in a reverse direction owing to the two secondary vortices newly generated at this region.

Figure 7 shows the effects of Ra, $\varepsilon$ and $\phi$ on the local Nusselt number along the surface of the outer cylinder $Nu_{loc}$. For all cases, as nanoparticle volume fraction increases, the value of local Nusselt number enhances. At Ra = $10^3$, the isotherms show almost a symmetric shape, with respect to the horizontal centerline, because the dominant heat transfer mechanism is conduction. As a result, the distribution of the local Nusselt numbers along the surface of the cold surface of the enclosure shows a symmetric shape. When we move from point A to B along the top wall of the enclosure, the local Nusselt number decreases and reaches a local minimum value close to zero at point B. When we move from point B to C along the right wall of the enclosure, the local Nusselt number increases, reaches a local maximum value, and decreases again until it has a local minimum value at point D. When we move further from point D to E, the local Nusselt number increases slightly again. The observed changes are most likely due to changes in thermal boundary layer thickness. The local minimum and maximum values of local Nusselt number occur at the same point of Ra = $10^3$ when Rayleigh number increases up to $10^4$, but the local Nusselt profiles are no longer symmetric. Because of the generation of thermal plumes, due to the domination of the convective heat transfer mechanism at high

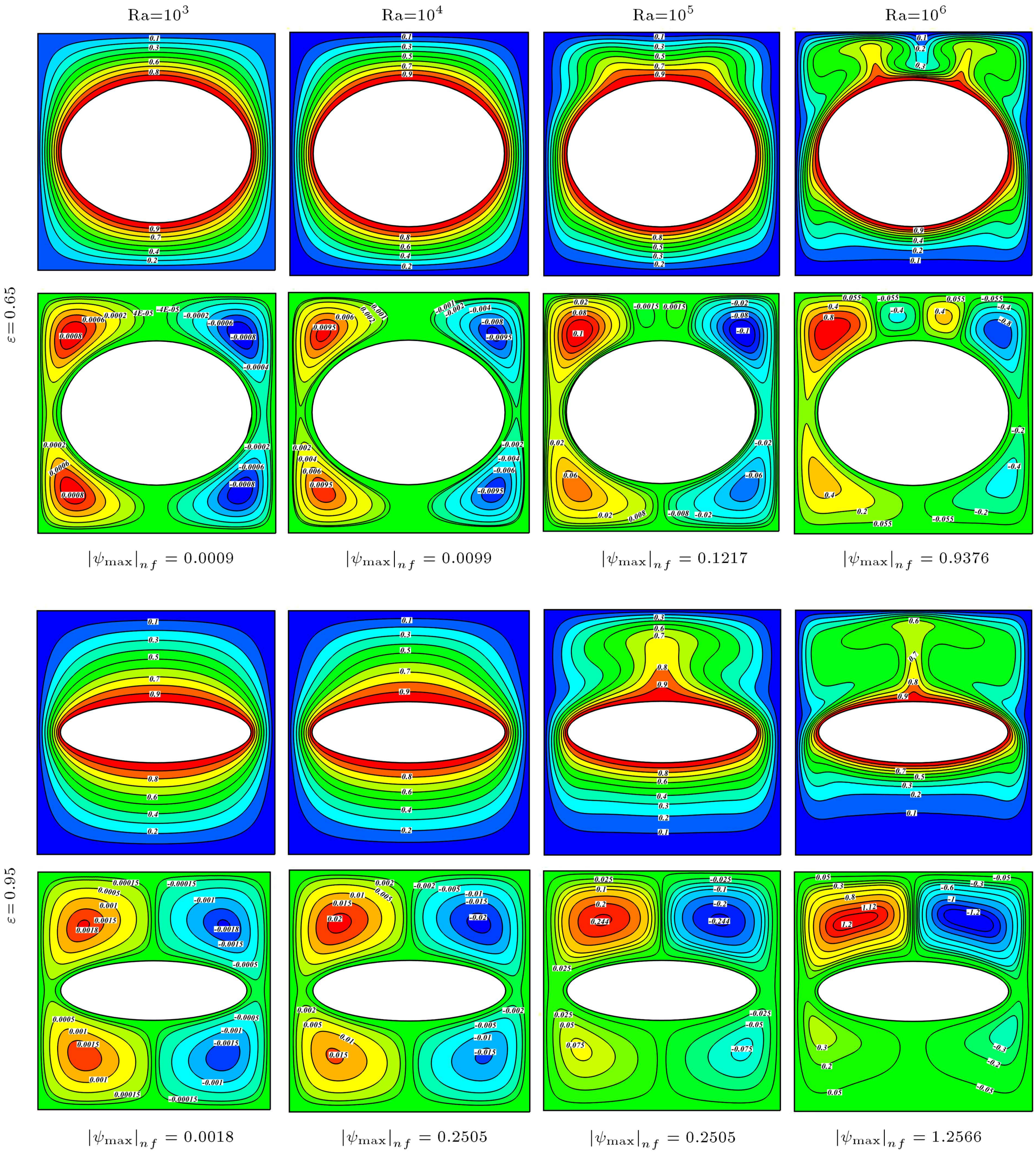


**Figure 6.** Effects of Ra and $\varepsilon$ on isotherms (up) and streamlines (down) contours for Cu-water case ($\phi = 0.06$).

Rayleigh numbers, local Nusselt number profiles have more extremum. It is interesting to notice that the local Nusselt number profile is more complex when Ra $= 10^6$ and $\varepsilon = 6.5$. This observation is due to the presence of three plumes in the vicinity of the top wall of the enclosure. By squeezing isotherms in the upper half of the enclosure, the primary plume is divided into three plumes. So, $\mathrm{Nu}_{loc}$ have one maximum and one minimum point between A and B. Also, in this case, there is one minimum point between B and D, which is due to domination of the conduction mechanism in this region.

Figure 8 shows the effects of Ra and $\varepsilon$ on average Nusselt number along the walls of the enclosure. Average Nusselt number has a direct relationship with Rayleigh number and the nanoparticle volume fraction, but has a reverse relationship with eccentricity.

The enhancement of heat transfer between the case of $\phi = 0.06$ and the pure fluid (base fluid) case is defined as:

$$\mathrm{En} = \frac{\overline{\mathrm{Nu}_{ave}}\,(\phi = 0.06) - \overline{\mathrm{Nu}_{ave}}\,(\text{base fluid})}{\overline{\mathrm{Nu}_{ave}}\,(\text{base fluid})} \times 100. \tag{23}$$

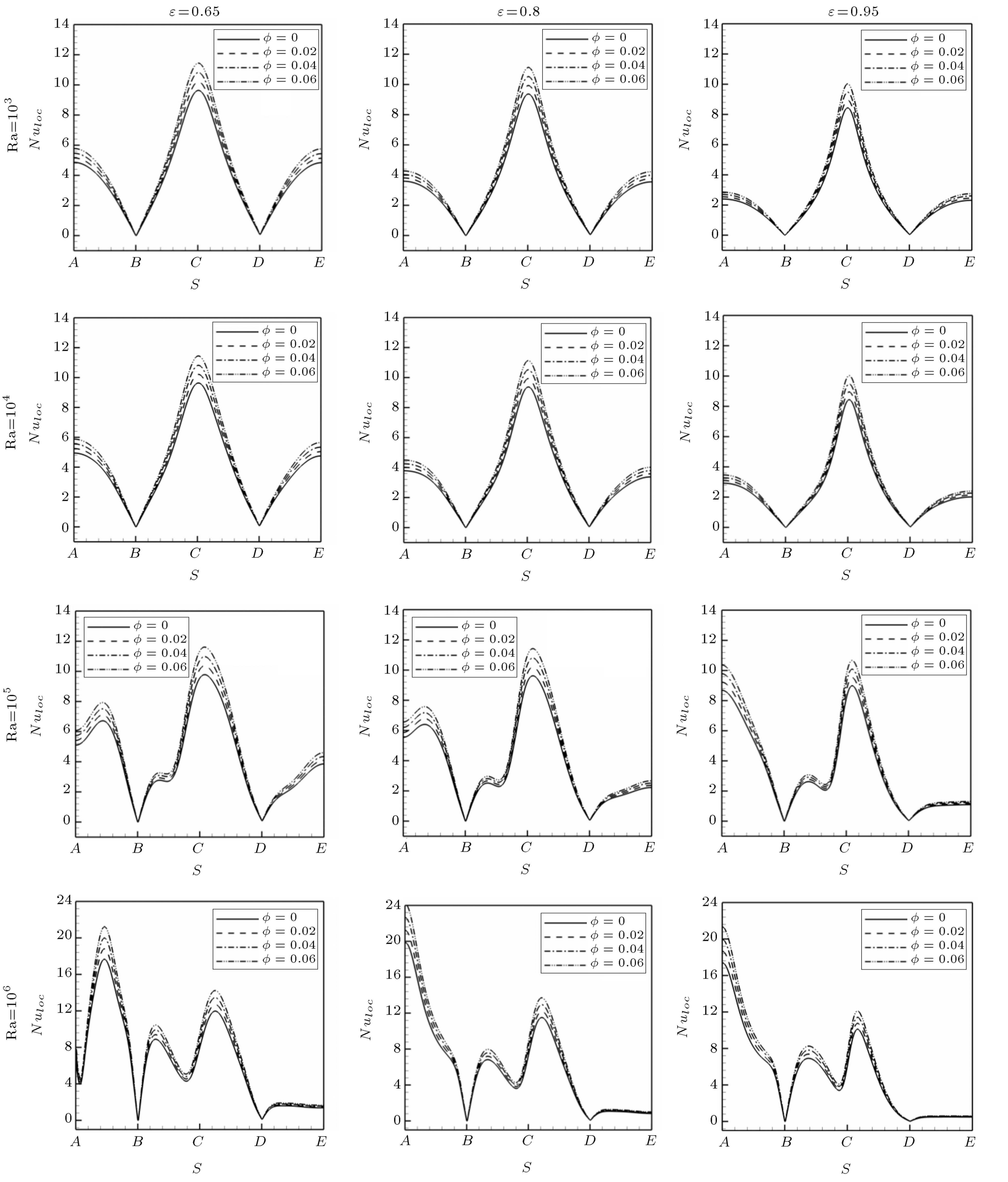


**Figure 7.** Effects of Ra, $\varepsilon$ and $\phi$ on local Nusselt number along the surface of the outer cylinder ($\mathrm{Nu_{loc}}$) for Cu-water case.

Effects of Ra and $\varepsilon$ ratio of enhancement of heat transfer, due to addition of nanoparticles, for the case of Cu-water, is shown in Figure 9. When $\varepsilon = 0.65$ and $\varepsilon = 0.8$, the effect of nanoparticles is more pronounced at low Rayleigh number than at high Rayleigh number domination of the conduction heat transfer mechanism. For $\varepsilon = 0.95$, enhancement of heat transfer decreases with increases in Rayleigh number when $\mathrm{Ra} \leq 10^5$, but decreases when $\mathrm{Ra} > 10^5$. When $\mathrm{Ra} = 10^3, 10^4$ and $10^6$, an increase in eccentricity leads to an increase in En, but for $\mathrm{Ra} = 10^5$, the opposite trend is observed.

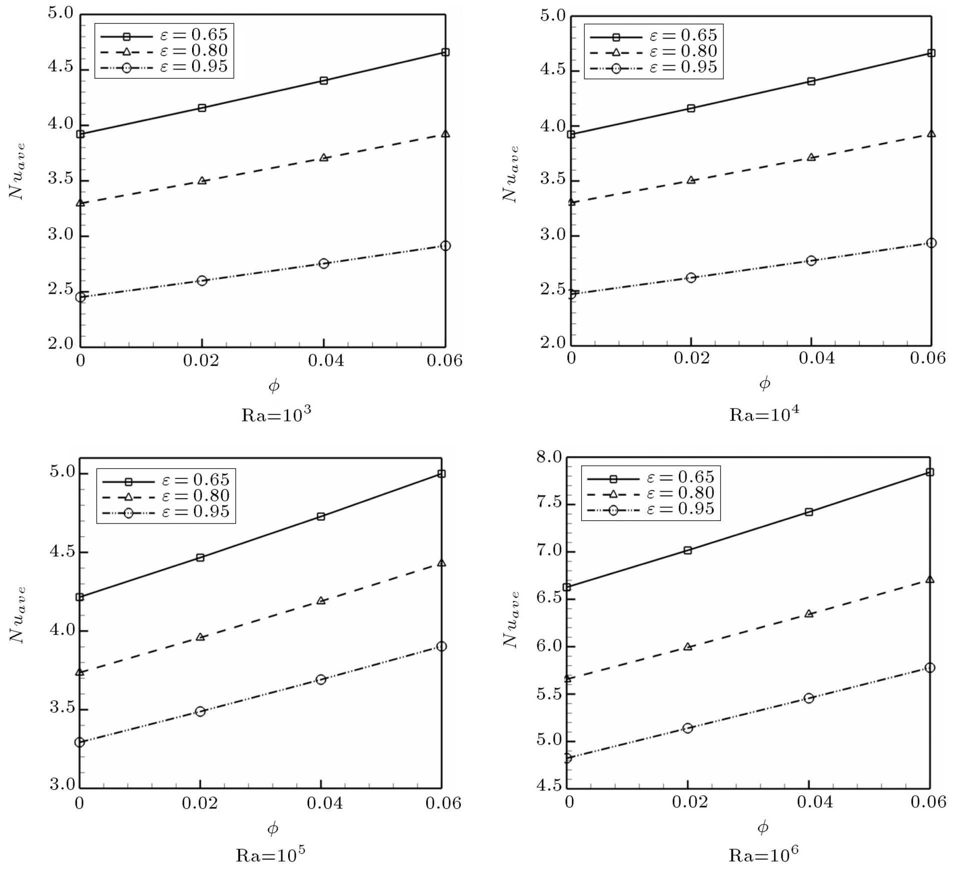


**Figure 8.** Effects of Ra and $\varepsilon$ on average Nusselt number along the walls of the enclosure ($\mathrm{Nu}_{ave}$).

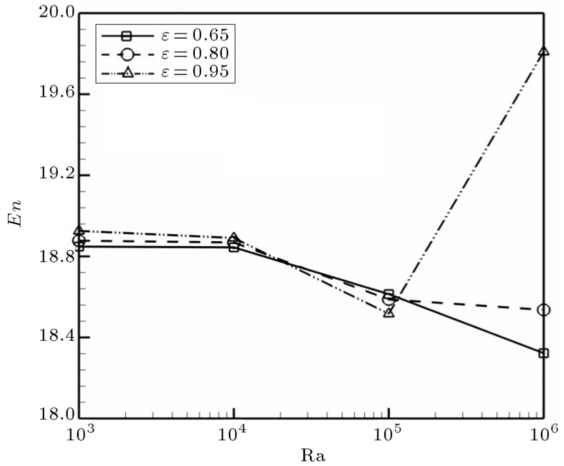


**Figure 9.** Effects of Ra and $\varepsilon$ on ratio of enhancement of heat transfer due to addition of nanoparticles for Cu-water case.

## 5. Conclusions

In this study, natural convection heat transfer in a concentric annulus between a cold outer square cylinder and a heated inner elliptic cylinder filled with nanofluid is investigated numerically using the LBM scheme. The effects of nanoparticle volume fraction, eccentricity and Rayleigh number on the flow and heat transfer characteristics have been examined. The results show that the average Nusselt number is an increasing function of nanoparticle volume fraction and Rayleigh number, while it is a decreasing function of eccentricity. Also, it can be found that the minimum value of enhancement of heat transfer occurs at $\varepsilon = 0.95$ for Ra $= 10^5$, but for other values of Rayleigh number, it is obtained at $\varepsilon = 0.65$.

## Nomenclature

| | |
|---|---|
| $a$ | The major axis of elliptic cylinder |
| $b$ | The minor axis of elliptic cylinder |
| $c$ | Lattice speed |
| $c_i$ | Discrete particle speeds |
| $C_p$ | Specific heat at constant pressure |
| $F$ | External forces |
| $f$ | Density distribution functions |
| $f^{eq}$ | Equilibrium density distribution functions |
| $g$ | Internal energy distribution functions |
| $g^{eq}$ | Equilibrium internal energy distribution functions |
| $g_y$ | Gravitational acceleration (m s$^{-2}$) |

| | |
|---|---|
| $k$ | Thermal conductivity |
| $L$ | Height or width of the enclosure |
| Nu | Nusselt number |
| $p$ | Pressure (Pa) |
| Pr | Prandtl number ($= \upsilon/\alpha$) |
| Ra | Rayleigh number ($= g\beta\Delta TL^3/\alpha\upsilon$) |
| $T$ | Fluid temperature |
| $(u, v)$ | Velocity components in $(x, y)$ directions, respectively |
| $(x, y)$ | Cartesian coordinates |
| $(X, Y)$ | Dimensionless coordinates |
| $w_i$ | Weighting factors |

***Greek symbols***

| | |
|---|---|
| $\alpha$ | Thermal diffusivity ($m^2s^{-1}$) |
| $\phi$ | Volume fraction |
| $\theta$ | Dimensionless temperature |
| $\mu$ | Dynamic viscosity ($Pas^{-1}$) |
| $\upsilon$ | Kinematic viscosity ($m^2s$) |
| $\rho$ | Fluid density ($kgm^{-3}$) |
| $\tau_c$ | Relaxation time for temperature |
| $\tau_v$ | Relaxation time for flow |
| $\beta$ | Thermal expansion coefficient ($K^{-1}$) |
| $\psi$ | Stream function |
| $\varepsilon$ | Eccentricity |

***Subscripts***

| | |
|---|---|
| $loc$ | Local |
| $ave$ | Average |
| $h$ | Hot |
| $c$ | Cold |
| $nf$ | Nanofluid |
| $f$ | Base fluid |
| $s$ | Solid particles |

## References


1. Choi, S.U.S. "Enhancing thermal conductivity of fluids with nanoparticles", *Developments and Applications of Non-Newtonian Flows,* D.A. Siginer and H.P. Wang, Eds., ASME, New York, **FED-231/MD-66**, pp. 99-105 (1995).
2. Khanafer, K., Vafai, K. and Lightstone, M. "Buoyancy-driven heat transfer enhancement in a two-dimensional enclosure utilizing nanofluids", *Int. J. Heat Mass Transfer,* **46**, pp. 3639-3653 (2003).
3. Oztop, H.F. and Abu-Nada, E. "Numerical study of natural convection in partially heated rectangular enclosures filled with nanofluids", *Int. J. of Heat and Fluid Flow,* **29**, pp. 1326-1336 (2008).
4. Abu-Nada, E. and Oztop, H.F. "Effects of inclination angle on natural convection in enclosures filled with Cu-water nanofluid", *Int. J. of Heat and Fluid Flow,* **30**, pp. 669-678 (2009).
5. Oztop, H.F., Mobedi, M., Abu-Nada, E. and Pop, I. "A heatline analysis of natural convection in a square inclined enclosure filled with a CuO nanofluid under non-uniform wall heating condition", *Int. J. of Heat and Mass Transfer*, **55**, pp. 5076-5086 (2012).
6. Sheikholeslami, M., Gorji-Bandpy, M., Ganji, D.D., Soleimani, S. "MHD natural convection in a nanofluid filled inclined enclosure with sinusoidal wall using CVFEM", *Neural Comput & Applic,* DOI 10.1007/s00521-012-1316-4 (2013).
7. Soleimani, S., Sheikholeslami, M., Ganji D.D. and Gorji-Bandpay, M. "Natural convection heat transfer in a nanofluid filled semi-annulus enclosure", *Int. Communications in Heat and Mass Transfer,* **39**, pp. 565-574 (2012).
8. Abu-Nada, E., Masoud, Z. and Hijazi, A. "Natural convection heat transfer enhancement in horizontal concentric annuli using nanofluids", *Int. Communications in Heat and Mass Transfer*, **35**, pp. 657-665 (2008).
9. Oztop, H.F., Abu-Nada, E., Varod, Y. and Al-Salem, Kh. "Computational analysis of non-isothermal temperature distribution on natural convection in nanofluid filled enclosures", *Super Lattices and Microstructures,* **49**, pp. 453-467 (2011).
10. Nemati, H., Farhadi, M., Sedighi, K., Ashorynejad, H.R. and Fattahi, E. "Magnetic field effects on natural convection flow of nanofluid in a rectangular cavity using the Lattice Boltzmann model", *Scientia Iranica B,* **19**(2), pp. 303-310 (2012).
11. Abu-Nada, E., Oztop, Hakan. F. and Pop, I. "Buoyancy induced flow in a nanofluid filled enclosure partially exposed to forced convection", *Superlattices and Microstructures*, **51**, pp. 381-395 (2012).
12. Sheikholeslami, M. and Ganji, D.D. "Heat transfer of Cu-water nanofluid flow between parallel plates", *Powder Technology*, **235**, pp. 873-879 (2013).
13. Sheikholeslami, M., Gorji-Bandpy, M. and Domairry, G. "Free convection of nanofluid filled enclosure using lattice Boltzmann method (LBM)", *Appl. Math. Mech.-Engl. Ed.*, **34**(7), pp. 1-15 (2013).
14. Ashorynejad, H.R., Sheikholeslami, M., Pop, I. and Ganji, D.D. "Nanofluid flow and heat transfer due to a stretching cylinder in the presence of magnetic field", *Heat Mass Transfer*, **49**, pp. 427-436 (2013).
15. Sheikholeslami, M., Gorji-Bandpy, M., Seyyedi, S.M., Ganji, D.D., Rokni, H.B. and Soleimani, S. "Application of LBM in simulation of natural convection in a nanofluid filled square cavity with curve boundaries", *Powder Technology*, doi: 10.1016/j.powtec.2013.06.008 (2013).
16. Ashorynejad, H.R., Mohamad, A.A. and Sheikholeslami, M. "Magnetic field effects on natural convection flow of a nanofluid in a horizontal cylindrical

annulus using Lattice Boltzmann method", *Int. J. of Thermal Sci.*, **64**, pp. 240-250 (2013).

17. Sheikholeslami, M., Hatami, M. and Ganji, D.D. "Analytical investigation of MHD nanofluid flow in a semi-porous channel", *Powder Technology*, doi: 10.1016/j.powtec.2013.05.030 (2013).

18. Sheikholeslami, M., Ganji, D.D., Ashorynejad, H.R. and Rokni, H.B. "Analytical investigation of Jeffery-Hamel flow with high magnetic field and nano particle by Adomian decomposition method", *Appl. Math. Mech.-Engl. Ed.*, **33**(1), pp. 1553-1564 (2012).

19. Sheikholeslami, M., Ashorynejad, H.R., Domairry, G. and Hashim, I. "Flow and heat transfer of Cu-water nanofluid between a stretching sheet and a porous surface in a rotating system", *Hindawi Publishing Corporation J. of Applied Mathematics*, Article ID 421320, 19 pages, doi:10.1155/2012/421320 (2012).

20. Shaija, A. and Narasimham, G.S.V.L. "Effect of surface radiation on conjugate natural convection in a horizontal annulus driven by inner heat generating solid cylinder", *Int. J. of Heat and Mass Transfer*, **52**, pp. 5759-5769 (2009).

21. Onyegegbu, S.O. "Heat transfer inside a horizontal cylindrical annulus in the presence of thermal radiation and buoyancy", *Int. J. Heat Mass Transfer*, **29**, pp. 659-671 (1986).

22. Sheikholeslami , M., Gorji-Bandpy, M., Ganji, D.D., Soleimani, S. and Seyyedi, S.M. "Natural convection of nanofluids in an enclosure between a circular and a sinusoidal cylinder in the presence of magnetic field", *Int. Communications in Heat and Mass Transfer,* **39**, pp. 1435-1443 (2012).

23. Haldar, S.C. "Combined convection in developing flow through a horizontal concentric annulus", *Numer. Heat Transf., A,* **34**(6), pp. 673-685 (1998).

24. Shu, C. and Zhu, Y.D. "Efficient computation of natural convection in a concentric annulus between an outer square cylinder and an inner circular cylinder", *Int. J. for Numerical Methods in Fluids,* **38**, pp. 429-445 (2002)

25. Yu, D., Mei, R., Luo, L.S. and Shyy, W. "Viscous flow computations with the method of lattice Boltzmann equation", *Progr. Aerospace Sci.*, **39**, pp. 329-367 (2003).

26. Succi, S., *The Lattice Boltzmann Equation for Fluid Dynamics and Beyond*, Clarendon Press, Oxford (2001).

27. Kao, P.H. and Yang, R.J. "Simulating oscillatory flows in Rayleigh-Benard convection using the lattice Boltzmann method", *Int. J. Heat Mass Transfer*, **50**, pp. 3315-3328 (2007).

28. Dixit, H.N. and Babu, V. "Simulations of high Rayleigh number natural convection in a square cavity using the lattice Boltzmann method", *Int. J. Heat Mass Transfer*, **49**, pp. 727-739 (2006).

29. Kefayati, GH.R., Gorji-Bandpy, M., Sajjadi, H. and Ganji, D.D. "Lattice Boltzmann simulation of MHD mixed convection in a lid-driven square cavity with linearly heated wall", *Scientia Iranica, B*, **19**(4), pp. 1053-1065 (2012).

30. Bararnia, H., Soleimani, S. and Ganji, D.D. "Lattice Boltzmann simulation of natural convection around a horizontal elliptic cylinder inside a square enclosure", *Int.Communications in Heat and Mass Transfer*, **38**, pp. 1436-1442 (2011).

31. Kefayati, G.H.R., Hosseinizadeh, S.F., Gorji, M. and Sajjadi, H. "Lattice Boltzmann simulation of natural convection in tall enclosures using water/$SiO_2$ nanofluid", *Int. Communications in Heat and Mass Transfer*, **38**(6), pp. 798-805 (2011).

32. Bararnia, H., Hooman, K. and Ganji, D.D. "Natural convection in a nanofluid filled portion cavity; the lattice-Boltzmann method", *Numerical Heat Transfer, Part A*, **59**, pp. 487-502 (2011).

33. Sheikholeslami, M., Gorji-Bandpay, M. and Ganji, D.D. "Magnetic field effects on natural convection around a horizontal circular cylinder inside a square enclosure filled with nanofluid", *Int. Communications in Heat and Mass Transfer,* **39**, pp. 978-986 (2012).

34. Sheikholeslami, M., Gorji-Bandpay, M., Ganji, D.D. and Soleimani, S. "Effect of a magnetic field on natural convection in an inclined half-annulus enclosure filled with Cu-water nanofluid using CVFEM", *Advanced Powder Technology*, doi.org/10.1016/j.apt.2013.01.012, (2013).

35. Sheikholeslami, M., Ganji, D.D. and Ashorynejad, H.R. "HYPERLINK "http://136.145.90. 90:2068/science/article/pii/S0032591013001149" Investigation of squeezing unsteady nanofluid flow using ADM", *Powder Technology*, **239**, pp. 259—265 (2013).

36. Sheikholeslami, M., Gorji-Bandpy, M. , Ganji, D.D. and Soleimani, S. "Natural convection heat transfer in a cavity with sinusoidal wall filled with CuO-water nanofluid in presence of magnetic field", *Journal of the Taiwan Institute of Chemical Engineers*, http://dx.doi.org/10.1016/j.jtice.2013.04.019 (2013).

37. Yan, Y.Y. and Zu, Y.Q. "Numerical simulation of heat transfer and fluid flow past a rotating isothermal cylinder A LBM approach", *International Journal of Heat and Mass Transfer*, **51**, pp. 2519-2536 (2008).

38. Xuan, Y. and Roetzel, W. "Conceptions for heat transfer correlation of nanofluids", *International Journal of Heat and Mass Transfer*, **43**(19), pp. 3701-3707 (2000).

39. Wang, X.Q. and Mujumdar, A.S. "Heat transfer characteristics of nanofluids: A review", *International Journal of Thermal Science*, **46**(1), pp. 1-19 (2007).

40. Moukalled, F. and Acharya, S. "Natural convection in the annulus between concentric horizontal circular and square cylinders", *Journal of Thermophysics and Heat Transfer*, **10**(3), pp. 524-531 (1996).

## Biographies

**Mohsen Sheikholeslami Kandelousi** received his BS degree from the Department of Mechanical Engineering at Mazandaran University, Iran, and his MS degree in the Energy Conversion subfield from the Department of Mechanical Engineering at Babol University of Technology, Babol, Iran, where he is currently a PhD degree student. His research interests include: CFD, mesoscopic modeling of fluid flow using LBM and Monte Carlo Methods, applications of nonlinear science in Mechanical Engineering.

**Mofid Gorji-Bandpy** received his PhD degree in Mechanical Engineering from the University of Wales College, Cardiff, UK, and is currently Professor of Mechanical Engineering at Babol Noshirvani University of Technology, Babol, Iran. His research interests include: fluid mechanics, turbomachinery (all hydro engineering subjects), renewable energy, water distribution networks, mechanics and thermodynamics of propulsion systems and internal combustion chambers.

**Davood Domiri Ganji** received his PhD degree in Mechanical Engineering from Tarbiat Modares University, Iran, and is currently Associate Professor of Mechanical Engineering at Babol Noshirvani University of Technology, Babol, Iran. His research interests include: nonlinear science in science and engineering, inverse problems and spray modeling.